Perfect transmission and self-similar optical transmission spectra in symmetric Fibonacci-class multilayers

X. Q. Huang,[1,2] S. S. Jiang,[1] R. W. Peng,[1] and A. Hu[1]
[1]*National Laboratory of Solid State Microstructures and Department of Physics, Nanjing University, Nanjing 210093, China*
[2]*Department of Telecommunication Engineering, Communication Engineering Institute of Nanjing, PLA University of Science and Technology, Nanjing 210016, China*
(Received 24 November 2000; published 22 May 2001)

We study the transmission properties of light through the symmetric Fibonacci-class [SFC(n)] quasiperiodic dielectric multilayers, which possess a mirror symmetry. For a normal incidence of light, many perfect transmission peaks (the transmission coefficients are unity) are numerically obtained. The transmission coefficient exhibits a two-cycle feature in a family of the SFC(n) with an odd n, while a three-cycle feature in another family with an even n. The scaling factors $f(n)$, which give a description of the self-similar behaviors of transmission spectra, are analytical obtained. Let $m_{ij}^{(n)}(k)$ $(i,j=1,2)$ be the elements of the total transfer matrix of the kth generation of SFC(n); it is proven that the positions (wavelength) of the perfect transmission peaks can be uniquely determined by $m_{12}^{(n)}(k)+m_{21}^{(n)}(k)=0$. The analytical results are very well confirmed by the numerical calculations.

DOI: 10.1103/PhysRevB.63.245104 PACS number(s): 42.25.Bs, 42.70.Qs, 61.44.Br

I. INTRODUCTION

The experimental discovery of quasicrystals by Shechtman *et al.*[1] has led to intense investigations of the structure and physical properties of deterministic aperiodic systems.[2–15] In the early days, the dominating part of the theoretical work had been focused on the electronic properties of the Fibonacci sequence.[2–5] In 1985, Merlin *et al.*[16] reported the fabrication of semiconducting and metallic quasiperiodic superlattices using the molecular-beam-epitaxy (MBE) technique. Afterwards, several interesting experimental studies have been reported.[17–19] These experimental works exhibit unusual properties that are very different from those of periodic and disordered systems.

Recently, there has been significant interest in studies of the localization of electromagnetic waves (EW) in photonic band-gap (PBG) materials.[20–24] This interest is partly due to the fact that the interactions between the electrons are not existent any more and the experiments can be performed at the room temperature. Furthermore, the unusual property of the control of the propagation of light in the PBG has potential applications in many optical devices. At the same time, studies on the PBG have been extended to photonic quasiperiodic structures, and some interesting results have been reported.[17,18,25–34] The photonic Fibonacci lattice was proposed by Kohmoto *et al.*[26] They predicted a fractal behavior of the transmission spectrum. Later, the experimental realization of optical Fibonacci dielectric multilayers has been reported.[18] In our opinion, the rich multifractal structures of transmission spectra of the quasiperiodic optical multilayers may provide a possible application of these systems as narrow-band filters. However, we have noted that the transmission coefficients of the mentioned works above are far below unity and it is still difficult to apply these results in real optical systems. On the other hand, Dunlap *et al.*[35] reported the delocalization-localization transition in the so-called one-dimensional (1D) random-dimer model (RDM). The basic reason for the appearance of extended electronic states in the RDM has been traced to the existence of symmetric internal structure.[36] Motivated by these investigations, recently we introduced the internal symmetric into a 1D binary Fibonacci dielectric multilayer. Surprisingly, many perfect transmission peaks are definitely found in the optical transmission spectra of the study system.[37] In the paper,[37] though, there is strong numerical evidence that optical perfect transmission phenomenon can be observed in the system, yet no satisfactory explanation of the physical nature of the results is provided and that a rigorous quantitative understanding of this phenomenon is still a problem to be solved. In this present paper, we will study in detail the optical transmission properties of light through the quasiperiodic multilayers that are arranged in the Fibonacci-class [FC(n)] sequences[38] along two opposite directions and that also possess a mirror symmetry. We will try to explain the general mechanism behind the numerical conclusions. In particular, we will show analytically where the perfect transmission peaks can be found in a given system and make comparisons between the theoretical results and the numerical calculations.

We organize this paper as follows. In Sec. II we introduce the models we are studying. In Sec. III we study the optical transmission properties of the studied models. Two-cycle and three-cycle behavior of transmission coefficients are theoretically predicted and numerically confirmed. The scaling factors $f(n)$ are also analytically obtained. Then, in Sec. IV, we theoretically predict the positions ($\lambda_0/2\lambda$, here λ_0 is the central wavelength) where the transmission coefficients are unity and perform numerical simulations. A brief summary is given in Sec. V.

II. MODEL

Let us consider a multilayer in which two types of layers A and B are arranged in a binary Fibonacci-class [FC(n)] sequence. Then, we can construct two kinds of binary sym-

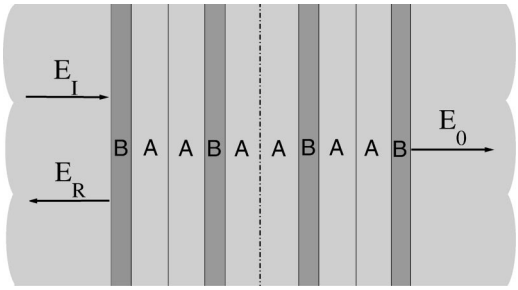

FIG. 1. Schematic representation of the SFC(1) multilayer, where E_I, E_R, and E_O are the input, reflective, and output electromagnetic fields, respectively.

metric Fibonacci-class [SFC(n)] sequences. For the jth generation of the SFC(n), these two symmetric sequences can be expressed as $S_j^{(n)}=\{G_j^{(n)},H_j^{(n)}\}$ and $P_j^{(n)}=\{H_j^{(n)},G_j^{(n)}\}$, where $G_j^{(n)}$ and $H_j^{(n)}$ are Fibonacci-class sequences; they obey the recursion relations

$$G_j^{(n)}=[G_{j-1}^{(n)}]^n G_{j-2}^{(n)}, \tag{1}$$

$$H_j^{(n)}=H_{j-2}^{(n)}[H_{j-1}^{(n)}]^n, \tag{2}$$

$$S_j^{(n)}=[G_{j-1}^{(n)}]^n G_{j-2}^{(n)} H_{j-2}^{(n)}[H_{j-1}^{(n)}]^n, \tag{3}$$

with $G_0^{(n)}=B, G_1^{(n)}=B^{n-1}A$, and $H_0^{(n)}=B, H_1^{(n)}=AB^{n-1}$. If we set $n=1$, the substitution rule (1) turns back to the Fibonacci case, and if $n=2$, it is exactly the intergrowth sequence.[29]

In this paper we will restrict ourselves to the case of $S_j^{(n)}$. As an example, the fourth sequence of $S_4^{(1)}$ is

$$S_4^{(1)}=\{BAABAABAAB\}. \tag{4}$$

The corresponding structure of (4) is shown in Fig. 1. As can be seen from this figure, the sequence has a mirror symmetry. For studying the transmission coefficient, we use the formalism presented in Ref. 26. For the SFC(n) with two different kinds of layers A and B, we denote the index of refraction by n_A and n_B and thickness by d_A and d_B, respectively. The incident monochromatic electromagnetic wave is supposed to be normal to the layer surfaces. For simplicity, the thickness of layers are chosen as $n_A d_A=n_B d_B$. Let matrices T_{AB} and T_{BA} represent the light propagation across interfaces $A \Leftarrow B$ and $B \Leftarrow A$, respectively. They are given by

$$T_{AB}=T_{BA}^{-1}=\begin{bmatrix}1 & 0\\ 0 & 1/R\end{bmatrix}, \tag{5}$$

where $R=n_A/n_B$, and the light propagation within layers A or B is described by matrix T_A and T_B, respectively. They can be presented by

$$T_A=T_B=\begin{bmatrix}\cos\delta & -\sin\delta\\ \sin\delta & \cos\delta\end{bmatrix}, \tag{6}$$

where the phase δ is given by $\delta=kn_A d_A=kn_B d_B$, and k is the vacuum wave vector. Now we consider the light propagation through a SFC(n) multilayer $S_j^{(n)}$, which is sandwiched by two medias of type A. There are $2F_j^{(n)}$ layers in $S_j^{(n)}$, where $F_{j+1}^{(n)}=nF_j^{(n)}+F_{j-1}^{(n)}$, for $j>2$, with $F_1^{(n)}=1$, $F_2^{(n)}=n$. The total transmission matrix of $S_j^{(n)}$ cannot be expressed as simple recursion relations, while each half part $H_j^{(n)}$ and $G_j^{(n)}$ can be expressed as

$$X_j^{(n)}=[X_{j-1}^{(n)}]^{n-1}X_{j-2}^{(n)}, \tag{7}$$

$$Z_j^{(n)}=Z_{j-2}^{(n)}[Z_{j-1}^{(n)}]^{n-1}, \tag{8}$$

where $X_j^{(n)}$ and $Z_j^{(n)}$ are the transmission matrices of $H_j^{(n)}$ and $G_j^{(n)}$, respectively. Therefore, the total transmission matrices of $S_j^{(n)}$ can be expressed as follows:

$$M_j^{(n)}=Z_j^{(n)}X_j^{(n)}=\begin{bmatrix}m_{11}^{(n)}(j) & m_{12}^{(n)}(j)\\ m_{21}^{(n)}(j) & m_{22}^{(n)}(j)\end{bmatrix}. \tag{9}$$

From this expression the transmission coefficient is given in terms of the matrix $M_j^{(n)}$ as

$$T[S_j^{(n)}]=\frac{4}{|M_j^{(n)}|^2+2}, \tag{10}$$

where $|M_j^{(n)}|^2$ denotes the sum of the squares of the four elements of $M_j^{(n)}$.

In the following investigation, we choose SiO_2 (A) and TiO_2 (B) as two elementary layers, with the indices of refraction of A and B as 1.45 and 2.3, respectively. The optical thickness of each layer is a quarter wavelength ($\lambda_0/4$), where λ_0 is the central wavelength. These conditions imply the phase $\delta=\pi\lambda_0/2\lambda$.

Here, we first briefly display the transmission coefficient as a function of δ/π for two different systems. Figures 2(a) and 2(b) show the numerical result for $FC(1)_6$ (13 layers) and $SFC(1)_6$ (26 layers), respectively. In Fig. 2(a), no perfect transmission peak can be found for the δ/π approximately belonging to the intervals [0.3,0.7]. It is of great interest to make a short comparison with the transmission of light through a multilayer with a mirror symmetry. From Fig. 2(b) it is clearly seen that the transmission coefficient behaves rather differently from that of Fig. 2(a). Many sharp transmission peaks with a unit transmission coefficient are shown in the figure. These results together seem to indicate that the symmetric internal structure can also influence the localization property of optical waves in a quasiperiodic optical system. In other words, the initially poor transmission of the optical wave can become a perfect transmission when the symmetric internal structure exists in the quasiperiodic optical multilayer. Following this section, we will extend our discussions to multilayers having different structure. The purpose of these investigations is to gain insight into this phenomenon.

III. SELF-SIMILAR TRANSMISSION SPECTRA

A. Analytical results

For the case of the ideal Fibonacci sequence [FC(1)], Kohmoto *et al.*[26] concluded the corresponding transfer matrices exist in a six-cycle property around $\delta/\pi=(m+\frac{1}{2})$,

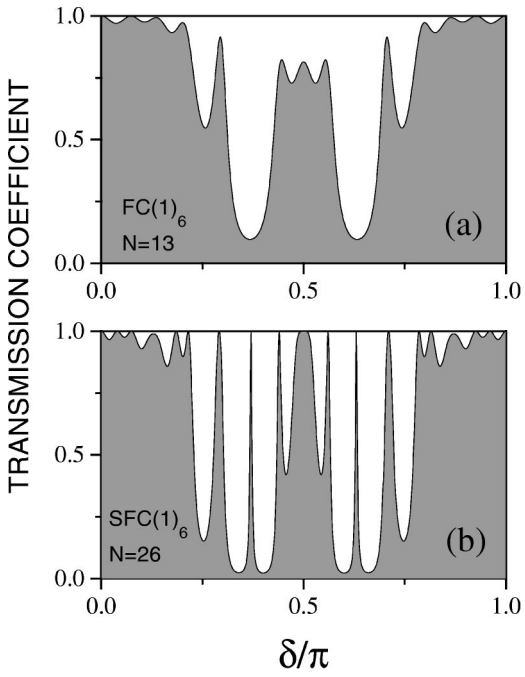

FIG. 2. The transmission coefficient versus δ/π for (a) $FC(1)_6$ (13 layers) and (b) $SFC(1)_6$ (26 layers), respectively. The indices of refraction are chosen as $n_A=1.45$ and $n_B=2.3$.

where m is an integer. For the case of a symmetric Fibonacci sequence [SFC(1)], we found that the $\delta/\pi=(m+\frac{1}{2})$ case also has a very special feature that the matrices satisfy[29]

$$M_{3k+1}^{(1)}=M_{3k+2}^{(1)}=-M_{3k+3}^{(1)}=-I, \quad k=0,1,2,\ldots, \tag{11}$$

where I is the unit matrix. Equation (11) can be rewritten as

$$M_j^{(1)}=(-I)^{F_j^{(1)}}, \quad j=0,1,2,\ldots, \tag{12}$$

where $F_j^{(1)}$ is the jth Fibonacci number. Generally, for a given $SFC(n)_j$, if the number of the layers $N=2F_j^{(n)}$, then at $\delta/\pi=0.5$ ($\lambda=\lambda_0$), the total transfer matrix may be expressed as

$$M_j^{(n)}=(-I)^{F_j^{(n)}}=(-I)^{nF_{j-1}^{(n)}+F_{j-2}^{(n)}}. \tag{13}$$

From this relation we can obtain the properties of the transfer matrices of different sequences at $\delta/\pi=0.5$. When n is even

$$M_j^{(n)}=(-I)^{F_{j-2}^{(n)}}=M_{j-2}^{(n)}. \tag{14}$$

Namely for the SFC(n) there is a two-cycle feature at $\delta/\pi=0.5$.

When n is odd, one has

$$\begin{aligned} M_j^{(n)}&=(-I)^{(n^2+1)F_{j-2}^{(n)}+nF_{j-3}^{(n)}} \\ &=(-I)^{nF_{j-3}^{(n)}}=(-I)^{F_{j-3}^{(n)}}=M_{j-3}^{(n)}. \end{aligned} \tag{15}$$

Namely, there is a three-cycle at $\delta/\pi=0.5$. Since the transmission matrix is I or $-I$, there must be perfect transmission at $\delta/\pi=0.5$ ($\lambda=\lambda_0$).

Kohmoto *et al.*[26] pointed out, around $\delta/\pi=0.5$, the scaling behavior of the transmission coefficient of FC(1) is characterized by the scale factor $f(1)=\sqrt{1+4[1+J(1)]^2}+2[1+J(1)]$, where the constant of motion $J(1)=(R^2-1)^2/4R^2$. In a recent paper,[37] we have performed a numerical simulation of the transmission coefficient of the SFC(1) and found that $f(1)$ and $J(1)$ can still be used to describe the scaling property of the corresponding transmission spectra. For this reason, in the following study we will mainly pay attention to the property of $X_j^{(n)}$.

We assume that $x_j(n)=\frac{1}{2}\mathrm{Tr}[X_{j+1}^{(n)}]$, $y_j(n)=\frac{1}{2}\mathrm{Tr}[X_j^{(n)}]$, and $z_j(n)=\frac{1}{2}\mathrm{Tr}[X_j^{(n)}X_{j+1}^{(n)}]$. Then, an invariant is as follows:[26,29,33]

$$\begin{aligned} J(n)&=x_j(n)^2+y_j(n)^2+z_j(n)^2-2x_j(n)y_j(n)z_j(n)-1 \\ &=\ldots \\ &=x_0(n)^2+y_0(n)^2+z_0(n)^2-2x_0(n)y_0(n)z_0(n)-1. \end{aligned} \tag{16}$$

By the use of the recursion relation (7), the first and second transfer matrices are, respectively, given by

$$\begin{aligned} X_1^{(n)}&=T_{AB}T_BT_{BA}, \\ X_2^{(n)}&=T_{AB}T_B^{n-1}T_{BA}T_A, \\ &=T_{AB}T_B^{n-2}T_{BA}T_{AB}T_BT_{BA}T_A=X_2^{(n-1)}X_1^{(n)}. \end{aligned} \tag{17}$$

Because the propagation matrices $X_j^{(n)}$ are all unimodular, when applying Eq. (17), one finds from the relation (16) that $J(n)$ is a constant which is given by

$$J=J(n)=J(n-1)=\cdots=J(1)=\sin^4\delta(R^2-1)^2/4R^2. \tag{18}$$

A proof is shown in the Appendix. The invariant of Eq. (18) is always positive and represents the strength of the effect of quasiperiodicity. By defining a three-dimensional vector $r_l=[x_l(n),y_l(n),z_l(n)]$, then

$$r_{l+1}=[x_{l+1}(n),y_{l+1}(n),z_{l+1}(n)]=T[x_l(n),y_l(n),z_l(n)].$$

In the renormalization-group point of view, the map T can be regarded as a scale transformation. The orbits given by successive iterations of T are confined on the two-dimensional manifold uniquely determined by R. When $n=1$, the nonlinear dynamical map is given explicitly by

$$r_{l+1}=T_1[r_l]=[z_l(1),x_l(1),2x_l(1)z_l(1)-y_l(1)].$$

The map T_1 has a six-cycle orbit given by[3]

$$\begin{aligned} A_s(0,0,a)&\rightarrow B_s(-a,0,0)\rightarrow C_s(0,-a,0)\rightarrow D_s(0,0,-a) \\ &\rightarrow E_s(a,0,0)\rightarrow F_s(0,a,0)\rightarrow A_s, \end{aligned} \tag{19}$$

where $a=\sqrt{1+J}$. Then A_s, B_s, C_s, D_s, E_s, and F_s are the fixed points of T_1^6. Linearization of T_1^6 around these fixed points yields the Jacobian matrix of the mapping. The eigen-

value of the linearized equation gives the scale factor $\alpha(1)$, which can be exactly calculated as

$$\alpha(1)=1+8a^4+4a^2\sqrt{1+4a^4}. \tag{20}$$

In fact, the two fixed points of T_1^6, A_s and D_s, are antipodal and A_s is mapped to D_s by three iterations. The rescaling parameter is called $f(1)$ which can be expressed as follows:[26]

$$f(1)=\sqrt{\alpha(1)}=2a^2+\sqrt{1+4a^4}. \tag{21}$$

When $n=2$, we obtain the following results:

$$\begin{aligned} x_{l+1}(2)&=2x_l(2)z_l(2)-y_l(2),\\ y_{l+1}(2)&=x_l(2),\\ z_{l+1}(2)&=2x_l(2)[2x_l(2)z_l(2)-y_l(2)]-z_l(2). \end{aligned} \tag{22}$$

Expressions (22) can also be written as a nonlinear dynamical map $r_{l+1}=T_2[r_l]$. Clearly, we have a four-cycle orbit,

$$A_p(0,a,0)\rightarrow B_p(a,0,0)\rightarrow C_p(0,-a,0)\rightarrow D_p(-a,0,9)\rightarrow A_p. \tag{23}$$

With linearization of T_2^4 around these fixed points (A_p, B_p, C_p, and D_p), one of the eigenvalues of the fixed points of period four is

$$\alpha(2)=1-16a^2+32a^4+4a(4a^2-1)\sqrt{4a^2-2}. \tag{24}$$

We note that, like the case T_1^6, A_p and C_p are antipodal and A_p is mapped to D_p by two iterations. Then the rescaling parameter is

$$f(2)=\sqrt{\alpha(2)}=(4a^2-1)+2a\sqrt{4a^2-2}. \tag{25}$$

When $n=3$, we have

$$\begin{aligned} x_{l+1}(3)&=2x(3)_l[2x_l(3)z_l(3)-y_l(3)]-z_l(3),\\ y_{l+1}(3)&=x_l(3),\\ z_{l+1}(3)&=8x_l(3)^3z_l(3)-4x_l(3)^2z_l(3)-4x_l(3)z_l(3)\\ &\quad+y_l(3). \end{aligned} \tag{26}$$

Equation (26) can be expressed as $r_{l+1}=T_3[r_l]$. It is easy to verify that the map T_3 also has the six-cycle orbit of Equation. (19). With the same analytical technique above, the rescaling factor $f(3)$ is obtained exactly and given by

$$f(3)=\tfrac{1}{2}(\sqrt{b-2}+\sqrt{b+2}) \quad \text{where}$$

$$b=2+784a^4-3584a^6+4096a^8. \tag{27}$$

We now turn to the case $n=4$ for which the nonlinear dynamical map is given by

$$\begin{aligned} x_{l+1}(4)&=8x_l(4)^3z_l(4)-4x_l(4)^2z_l(4)-4x_l(4)z_l(4)\\ &\quad+y_l(4),\\ y_{l+1}(4)&=x_l(4),\\ z_{l+1}(4)&=16x_l(4)^4z_l(4)-8x_l(4)^3z_l(4)-12x_l(4)^2z_l(4)\\ &\quad+4x_l(4)y_l(4)+z_l(4). \end{aligned} \tag{28}$$

From the above expressions, we can define a renormalization map T_4 which has the four-cycle orbit of Eq. (23). Consequently, the rescaling factor $f(4)$ is

$$f(4)=\frac{1}{2}(\sqrt{c-2}+\sqrt{c+2}) \quad \text{where}$$

$$c=2+576a^4-2304a^6+2304a^8. \tag{29}$$

We have derived the recursion relation of the dynamical maps of the FC(n) for several special cases ($n=1,2,3,4$). It is rather straightforward to prove that the FC(n) can be divided into two kinds: n is odd and n is even. The six-cycle fixed points for odd n and four-cycle fixed points for even n are the common properties. It should be noted that, in the following study, the obtained rescaling factors $f(n)$ ($n=1,2,3,4$) will be applied to describe the self-similar properties of transmission spectra of the symmetric Fibonacci-class multilayers.

B. Numerical results

To illustrate the scaling properties of the transmission spectra of the SFC(n), we numerically study the transmission coefficients for $\{[\mathrm{SFC}(1)_{12},\mathrm{SFC}(1)_{15}]\}$, $\{[\mathrm{SFC}(3)_6,\mathrm{SFC}(3)_9]\}$, and $\{[\mathrm{SFC}(2)_8,\mathrm{SFC}(2)_{10}]$, $[\mathrm{SFC}(4)_5,\mathrm{SFC}(4)_7]\}$. The main results are shown in Figs. 3 and Figs. 4 for two different families of the SFC(n) (odd n and even n), respectively. Figures 3(a) and 3(b) show the transmission spectra of the 12th and 15th generation of the SFC(1) around δ/π, respectively. It is clearly seen that these two figures are similar except for the scaling. This conclusion is also true for the 6th and 9th generation of the SFC(3) [see Figs. 3(c) and 3(d)]. Furthermore, Figs. 3 confirm that, when n is odd, the transmission spectra of the SFC(n) are similar with a three-cycle orbit about the δ/π. In Fig. 4 we show the transmission coefficient for another family of SFC(n) (n is even) with $n=2$ and 4, respectively. When $n=2$, the 8th (816 layers) and 10th (4656 layers) generation of quasiperiodic optical multilayers are studied. For the case of $n=4$, we chose the fifth (610 layers) and seventh (10946) generation of the optical sequences. The self-similar properties are also demonstrated clearly in these figures. Note the generation change of the chosen sequences in these figures; then, their similarity well confirms the above theoretical prediction of the two-cycle orbit of the transmission coefficient of SFC($2m$), where $m=1,2,\ldots$. Recall that the self-similarity of the transmission coefficients of the FC(1) is six cycle at $\delta/\pi=0.5$,[26] and the FC(2) is quasi-four-cycle.[29] The discrepancy is caused by the symmetry. The scaling is also displayed in these two figures. From Figs. 3 we have the scaling factors $f(1)=(0.5165-0.5)/(0.503\,25-0.5)\approx 5.076\,92$ and $f(3)=(0.5059-0.5)/(0.500\,095-0.5)\approx 62.105\,26$ for SFC(1) and SFC(3), respectively. We also

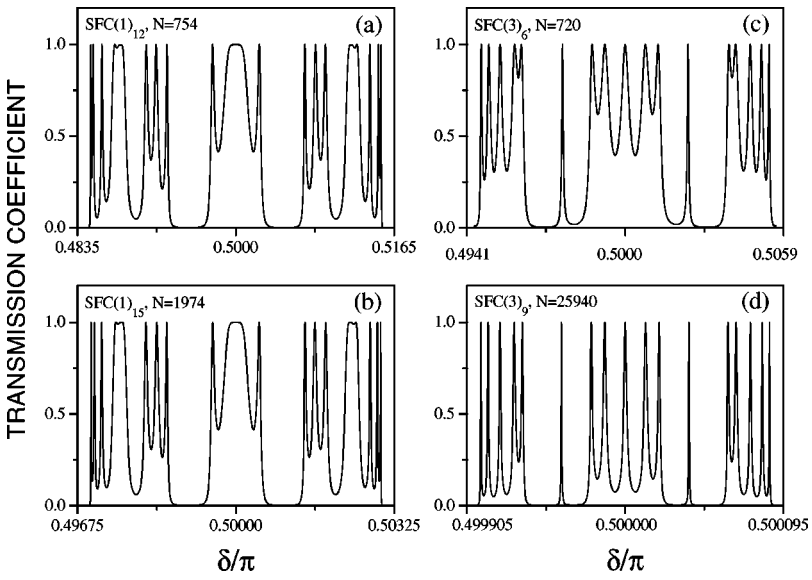

FIG. 3. The transmission coefficient versus δ/π for a family of SFC(n) with odd n. (a) and (b) for the case $n=1$, (c) and (d) for the case $n=3$, respectively.

respectively obtain the scaling factors of SFC(2) [Figs. 4(a) and 4(b)] and SFC(4) [Figs. 4(c) and 4(d)]. They are $f(2)=(0.5055-0.5)/(0.500715-0.5)\approx 7.692\,31$ and $f(4)=(0.5059-0.5)/(0.500\,142-0.5)\approx 41.549\,30$. These numerical results are well predicated by our analytical results of Eqs. (21), (25), (27), and (29). As can be seen, when $R=n_B/n_A$ is given, the invariant $J=J(n)=\sin^4\delta(R^2-1)^2/4R^2$ is the same for all the SFC(n) at the central wavelength (corresponds to $\delta/\pi=0.5$). For $n_A=1.45, n_B=2.3$, we obtain $J\approx 0.228\,375$ and the scaling factors can be obtained by calculating Eqs. (21), (25), (27), and (29). They are $f(1)\approx 2.456\,75+\sqrt{7.035\,62}\approx 5.109\,22$, $f(2)\approx 3.9135+2.2135\sqrt{2.9135}\approx 7.697\,28$, $f(3)\approx 0.5(\sqrt{3865.79}+\sqrt{3869.79})\approx 62.1947$, and $f(4)\approx 0.5(\sqrt{1844.4}+\sqrt{1848.4})\approx 42.97211$ for the SFC(1), SFC(2), SFC(3), and SFC(4), respectively.

IV. POSITIONS OF PERFECT TRANSMISSION PEAKS

From the form of Eq. (10) it is clear that the transmission coefficient is determined entirely by the properties of the matrix $M_j(n)$. Hence, in order to gain a deep insight into the physical implication of the numerical results in Figs. 2, 3, and 4, it is instructive to analyze the transfer matrices $X_j(n)$, $Z_j(n)$, and $M_j(n)$. In this section we restrict ourselves to the optical system of SFC(1). From Eqs. (5)–(8), the transfer matrices $X_j(n)$ and $Z_j(n)$ are, respectively, given by

$$X_0^{(1)}=\begin{bmatrix}\cos\delta & -R\sin\delta\\ \dfrac{\sin\delta}{R} & \cos\delta\end{bmatrix},\quad X_1^{(1)}=\begin{bmatrix}\cos\delta & -\sin\delta\\ \sin\delta & \cos\delta\end{bmatrix},$$

$$X_2^{(1)}=\begin{bmatrix}\cos^2\delta-\dfrac{\sin^2\delta}{R} & -(1+R)\cos\delta\sin\delta\\ \left(1+\dfrac{1}{R}\right)\cos\delta\sin\delta & \cos^2\delta-R\sin^2\delta\end{bmatrix},\ \ldots, \tag{30}$$

and

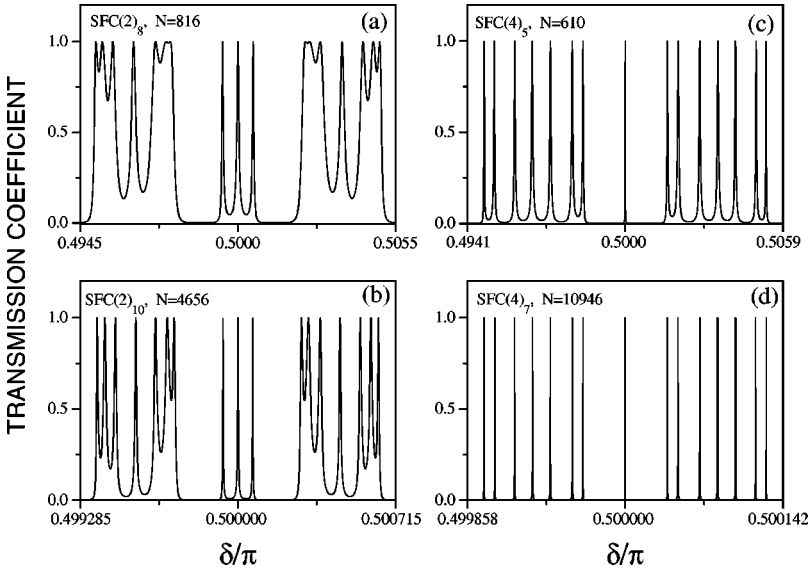

FIG. 4. The transmission coefficient versus δ/π for a family of SFC(n) with even n. (a) and (b) for the case $n=2$, (c) and (d) for the case $n=4$, respectively.

$$Z_0^{(1)}=X_0^{(1)},\quad Z_1^{(1)}=X_1^{(1)},$$

$$Z_2^{(1)}=\begin{bmatrix}\cos^2\delta-R\sin^2\delta & -(1+R)\cos\delta\sin\delta\\ \left(1+\frac{1}{R}\right)\cos\delta\sin\delta & \cos^2\delta-\frac{\sin^2\delta}{R}\end{bmatrix},\ \ldots. \tag{31}$$

If we write the matrices of Eq. (30) in a general form

$$X_j^{(1)}=\begin{bmatrix}C & D\\ E & F\end{bmatrix}, \tag{32}$$

where C, D, E, and F are four elements of $X_j^{(1)}$, then it can be shown that $Z_j^{(1)}$ can be represented by these four elements as

$$Z_j^{(1)}=\begin{bmatrix}F & D\\ E & C\end{bmatrix}. \tag{33}$$

The total transfer matrix $M_j^{(1)}$ can now be rewritten by substituting Eqs. (32) and (33) in Eq. (9),

$$M_j^{(1)}=Z_j^{(1)}X_j^{(1)}=\begin{bmatrix}CF+DE & 2DF\\ 2CE & CF+DE\end{bmatrix}.$$

It can then be seen that the diagonal elements of $M_j^{(1)}$ satisfy

$$m_{11}^{(1)}(j)=m_{22}^{(1)}(j). \tag{34}$$

By using the condition $\det|M_j^{(1)}|=1$, it is not difficult to prove that the standard expression of Eq. (10) will be determined by a relation involving only the off-diagonal elements. For the $S_j^{(1)}$, the expression of $T[S_j^{(1)}]$ is then

$$T[S_j^{(1)}]=\frac{4}{[m_{12}^{(1)}(j)+m_{21}^{(1)}(j)]^2+4}. \tag{35}$$

It follows directly from Eq. (35) that the reflection coefficient will vanish only when

$$m_{12}^{(1)}(j)+m_{21}^{(1)}(j)=0. \tag{36}$$

We should point out that Eq. (36) is the key expression in the following study. In fact, Eq. (35) can be applied quite generally to any kind of one-dimensional optical multilayers with a mirror symmetric.

In what follows, the above-obtained formula (36) will be applied to the symmetric Fibonacci multilayers constructed according to the substitution rule (3) of $n=1$. Consider first the second generation SFC(1), which is arranged as $BAAB$ and the corresponding total transfer matrix is given by

$$M_2^{(1)}=\begin{bmatrix}m_{11}^{(1)}(2) & m_{12}^{(1)}(2)\\ m_{21}^{(1)}(2) & m_{22}^{(1)}(2)\end{bmatrix}=\begin{bmatrix}\frac{(1+R)^2\cos4\delta-(R-1)^2}{4R} & -\frac{[(1+R)^2\cos2\delta+R^2-1]\sin2\delta}{2R}\\ \frac{[(1+R)^2\cos2\delta+1-R^2]\sin2\delta}{2R} & \frac{(1+R)^2\cos4\delta-(R-1)^2}{4R}\end{bmatrix}, \tag{37}$$

such that the sum of the off-diagonal elements of Eq. (37) can be explicitly written as

$$m_{12}^{(1)}(2)+m_{21}^{(1)}(2)=\frac{(1-R^2)\sin2\delta}{R}. \tag{38}$$

From Eqs. (36) and (38) it is evident that, when $R\neq1$, the condition for the existence of perfect transmission coefficients is entirely determined by $\sin2\delta=0$. As a result, the corresponding phases δ are

$$\delta_k(2)=k\pi/2,\quad k=0,1,2,\ldots. \tag{39}$$

If the phase δ is expressed in units of π, for the phase δ in the interval [1,2], three phases which uniquely determine the positions of the perfect transmission peaks are given by

$$P_k(2)=\delta_k(2)/\pi=k/2,\quad k=0,1,2. \tag{40}$$

This result is exemplified in Fig. 5(a), where the solid line is the numerical result and the analytical results of Eq. (40) are indicated by chain lines in this figure.

To have a better understanding of this technique and to emphasize the role played by the off-diagonal elements of the transfer matrix of the optical multilayers with a mirror symmetry, we shall apply it to the exactly soluble $\mathrm{SFC}(1)_4$. Similarly, in this case, the associated off-diagonal elements are given by

$$m_{12}^{(1)}(4)=-\frac{\sin2\delta}{16R^3}[A_1+4+B_1\cos2\delta+C_1\cos4\delta]\times[A_1+4R-B_1R\cos2\delta+C_1\cos4\delta], \tag{41}$$

$$m_{21}^{(1)}(4)=\frac{\sin2\delta}{16R^3}[A_1+4R^2-B_1R\cos2\delta+C_1\cos4\delta]\times[A_1+4R^3+B_1R^2\cos2\delta+C_1\cos4\delta], \tag{42}$$

where $A_1=-R^3+R^2+R-1$, $B_1=-4(1+R)$, and $C_1=(1+R)^3$. Consequently, the sum of two off-diagonal elements can be expressed as

$$m_{12}^{(1)}(4)+m_{21}^{(1)}(4)=\frac{(R^2-1)\sin2\delta}{8R^3}[A_2+B_2\cos2\delta+C_2\cos4\delta+D_2\cos6\delta], \tag{43}$$

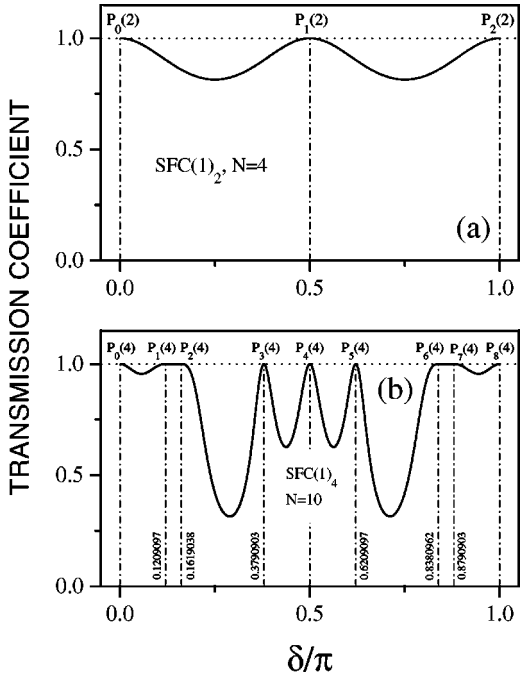

FIG. 5. The transmission coefficient versus δ/π for (a) $\mathrm{SFC}(1)_2$ (four layers) and (b) $\mathrm{SFC}(1)_4$ (ten layers), respectively. The chain lines are the theoretical results of resonant positions.

where $A_2=2-4R+4R^2-4R^3+2R^4$, $B_2=-(1+R)^2(1-6R+R^2)$, $C_2=-2(1+R)^2(1+R^2)$, and $D_2=(1+4R+6R^2+4R^3+R^4)$. From Eqs. (36) and (43), for a given R, there exist some special values of phase δ where the electromagnetic waves corresponding to these phases are transparent with unit transmission coefficients. These special values of δ are the solutions of the following equation:

$$\left[\cos 2\delta-\frac{1+R^2}{(1+R)^2}\right]\left[\cos^2 2\delta-\frac{1+R^2}{(1+R)^2}\right]\sin 2\delta=0. \tag{44}$$

If $\pi\leqslant\delta\leqslant 2\pi$, from the above equation one can obtain eight solutions that directly determine the positions of resonant peaks. These positions are

$$P_0(4)=0.0, \tag{45}$$

$$P_1(4)=\frac{\arccos[\sqrt{1+R^2}/(1+R)]}{2\pi},$$

$$P_2(4)=\frac{\arccos[(1+R^2)/(1+R)^2]}{2\pi},$$

$$P_3(4)=\frac{1}{2}-\frac{\arccos[\sqrt{1+R^2}/(1+R)]}{2\pi},$$

$$P_4(4)=0.5,$$

$$P_5(4)=\frac{1}{2}+\frac{\arccos[\sqrt{1+R^2}/(1+R)]}{2\pi},$$

$$P_6(4)=1-\frac{\arccos[(1+R^2)/(1+R)^2]}{2\pi},$$

$$P_7(4)=1-\frac{\arccos[\sqrt{1+R^2}/(1+R)]}{2\pi},$$

$$P_8(4)=1.0.$$

When $R=n_B/n_A=1.45/2.3\approx 0.630\,437\,8$, we have eight resonant peaks at

$$P_0(4)=0.0,$$

$$P_1(4)\approx\arccos(0.725\,043\,7)/2\pi\approx 0.120\,909\,7,$$

$$P_2(4)\approx\arccos(0.525\,688\,4)/2\pi\approx 0.161\,903\,8,$$

$$P_3(4)=0.5-P_1(4)\approx 0.379\,090\,3,$$

$$P_4(4)=0.5,$$

$$P_5(4)=0.5+P_1(1)=0.620\,909\,7,$$

$$P_6(4)=1.0-P_2(4)\approx 0.838\,069\,2,$$

$$P_7(4)=1.0-P_1(4)\approx 0.879\,090\,3,$$

and

$$P_8(4)=1.0.$$

By applying Eq. (10) again, we calculate the transmission coefficient as a function of δ/π for the fourth generation of the SFC(1). As shown in Fig. 5(b), our numerical result (solid line) agrees very well with the theoretical predictions (chain lines).

V. SUMMARY

We have studied the light-waves propagation in the symmetric Fibonacci-class quasiperiodic dielectric multilayers. We have shown that the symmetric internal structure in one-dimensional quasiperiodic systems can greatly enhance the transmission intensity. The scaling properties are retained in all the symmetric Fibonacci-class sequences; it demonstrates that in the transmission spectra, the quasiperiodicity is still deterministic. But the perfect transmission and the periodicity about the central wavelength demonstrate that the symmetry is an important factor. These two factors influence each other and cause rich structures of the transmission spectra. These phenomena will find their applications in the fabrication of the multiwavelength narrow-band optical filters. The experimental verification of these properties of electromagnet waves in the $\mathrm{SFC}(n)$ is in process.

ACKNOWLEDGMENTS

This project was supported by National Natural Science Foundation of China, the China Postdoctoral Science Foundation, the State Key Program for Basic Research from the

Ministry of Science and Technology of China, and in part by the Sanzhu Co. Ltd in Shandong. One of the authors (X.H.) would like to thank Dr. Y. Wang and S. F. Cheng for their helpful discussions.

APPENDIX: THE INVARIANT OF THE TRACE MAP

In this appendix we shall prove Eq. (18). First, using the definitions: $x_j(n)=\frac{1}{2}\mathrm{Tr}[X_{j+1}^{(n)}]$, $y_j(n)=\frac{1}{2}\mathrm{Tr}[X_j^{(n)}]$, and $z_j(n)=\frac{1}{2}\mathrm{Tr}[X_j^{(n)}X_{j+1}^{(n)}]$, then, $J(n)$ of Eq. (16) is given by

$$\begin{aligned}4J(n)+4=&\mathrm{Tr}^2[X_1^{(n)}]+\mathrm{Tr}^2[X_2^{(n-1)}X_1^{(n)}]\\&+\mathrm{Tr}^2[X_1^{(n)}X_2^{(n-1)}X_1^{(n)}]\\&-\mathrm{Tr}[X_1^{(n)}]\mathrm{Tr}[X_2^{(n-1)}X_1^{(n)}]\mathrm{Tr}[X_1^{(n)}X_2^{(n-1)}X_1^{(n)}].\end{aligned}\tag{A1}$$

From Eq. (17), we have an initial condition

$$X_1^{(n)}=X_1^{(n-1)}=\cdots=X_1^{(1)}=X_1,$$
$$X_2^{(n)}=X_2^{(n-1)}X_1.\tag{A2}$$

Substituting these into Eq. (A1), one gets

$$\begin{aligned}4J(n)+4=&\mathrm{Tr}^2[X_1]+\mathrm{Tr}^2[X_2^{(n-2)}X_1^2]+\mathrm{Tr}[X_2^{(n-1)}X_1^2]\\&\times\{\mathrm{Tr}[X_2^{(n-1)}X_1^2]-\mathrm{Tr}[X_1]\mathrm{Tr}[X_2^{(n-1)}X_1]\}.\end{aligned}\tag{A3}$$

Using the following relations:

$$\mathrm{Tr}(\mathbf{ab}^{-1})=\mathrm{Tr}(\mathbf{a})\mathrm{Tr}(\mathbf{b})-\mathrm{Tr}(\mathbf{ab}),$$
$$\mathrm{Tr}(\mathbf{ab}^2)=\mathrm{Tr}(\mathbf{ab})\mathrm{Tr}(\mathbf{b})-\mathrm{Tr}(\mathbf{a})$$

(valid for any 2×2 unimodular matrices **a** and **b**), Eq. (A3) can easily be rewritten as

$$\begin{aligned}4J(n)+4=&\mathrm{Tr}^2[X_1]+\mathrm{Tr}^2[X_2^{(n-2)}X_1^2]\\&-\mathrm{Tr}[X_2^{(n-1)}X_1^2]\mathrm{Tr}[X_2^{(n-1)}]\\=&\mathrm{Tr}^2[X_1]+\mathrm{Tr}^2[X_2^{(n-2)}X_1^2]\\&-\{\mathrm{Tr}[X_2^{(n-1)}X_1]\mathrm{Tr}[X_1]\\&-\mathrm{Tr}[X_2^{(n-1)}]\}\mathrm{Tr}[X_2^{(n-1)}]\\=&\mathrm{Tr}^2[X_1]+\mathrm{Tr}^2[X_2^{(n-1)}]+\mathrm{Tr}^2[X_2^{(n-2)}X_1^2]\\&-\mathrm{Tr}[X_1]\mathrm{Tr}[X_2^{(n-1)}]\mathrm{Tr}[X_2^{(n-2)}X_1^2]\\=&4J(n-1)+4.\end{aligned}$$

And finally we obtain

$$J(n)=J(n-1)=\cdots=J(1)=\sin^4\delta(R^2-1)^2/4R^2.\tag{A4}$$

From Eq. (A4) one finds that, for the normal incidence of light ($\delta=\pi/2$), the recurrence relation of $J(n)$ is determined only by the physical properties of chosen optical materials.

[1] D.S. Shechtman, I. Blech, D. Gratias, and J.W. Cahn, Phys. Rev. Lett. **53**, 1951 (1984).
[2] Q. Niu and F. Nori, Phys. Rev. Lett. **57**, 2070 (1986).
[3] M. Kohmoto, L.P. Kadanoff, and C. Tang, Phys. Rev. Lett. **50**, 1870 (1983).
[4] Y.Y. Liu and R. Riklund, Phys. Rev. B **35**, 6034 (1986).
[5] G. Gumbs and M.K. Ali, J. Phys. A **22**, 951 (1989).
[6] V. Kumar and G. Ananthakrishna, Phys. Rev. Lett. **59**, 1476 (1987).
[7] T. Fujiwara, M. Kohmoto, and T. Tokihiro, Phys. Rev. B **40**, 7413 (1989).
[8] J.M. Luck, Phys. Rev. B **39**, 5834 (1989).
[9] K. Iguchi, Phys. Rev. B **43**, 5915 (1991); J. Math. Phys. **33**, 3938 (1992); Int. J. Mod. Phys. B **8**, 1931 (1994); **11**, 2157 (1997).
[10] A. Hu, Z.X. Wen, S.S. Jiang, W.T. Tong, R.W. Peng, and D. Feng, Phys. Rev. B **48**, 829 (1993).
[11] X. Huang and C. Gong, Phys. Rev. B **58**, 739 (1998).
[12] E. Macia, Phys. Rev. B **60**, 10 032 (1999).
[13] A. Ghosh and S.N. Karmakar, Phys. Rev. B **61**, 1051 (2000).
[14] R. Oviedo-Roa, L.A. Perez, and C.M. Wang, Phys. Rev. B **62**, 13 805 (2000).
[15] X.G. Wang, U. Grimm, and M. Schreiber, Phys. Rev. B **62**, 14 020 (2000).
[16] R. Merlin, K. Bajema, R. Clarke, F.Y. Juang, and P.K. Bhattacharya, Phys. Rev. Lett. **55**, 1765 (1985).
[17] L. Chow and K.H. Guenther, J. Opt. Soc. Am. A **10**, 2231 (1993).
[18] W. Gellermann, M. Kohomoto, B. Sutherland, and P.C. Tayler, Phys. Rev. Lett. **72**, 633 (1994).
[19] S.N. Zhu, Y.Y. Zhu, and N.B. Ming, Science **278**, 843 (1997).
[20] S. John, Phys. Rev. Lett. **53**, 2169 (1984).
[21] S. John, Phys. Today **44**(5), 32 (1991).
[22] S. John and J. Wang, Phys. Rev. B **43**, 12 772 (1991).
[23] E. Yablonovitch, Phys. Rev. Lett. **58**, 2059 (1987).
[24] S. Noda, K. Tomoda, N. Yamamoto, and A. Chutinan, Science **289**, 604 (2000).
[25] M.S. Kushwaha, Int. J. Mod. Phys. B **10**, 977 (1996).
[26] M. Kohmoto, B. Sutherland, and K. Iguchi, Phys. Rev. Lett. **58**, 2436 (1987).
[27] M. Dulea, M. Severin, and R. Riklund, Phys. Rev. B **42**, 80 (1990).
[28] K. Iguchi, Mater. Sci. Eng., B **15**, L13 (1992).
[29] X.Q. Huang, Y.Y. Liu, and D. Mo, Solid State Commun. **87**, 601 (1993).
[30] T. Hattori, N. Tsurumachi, S. Kawato, and H. Nakatsuka, Phys. Rev. B **50**, 4220 (1994).
[31] Y.S. Chan, C.T. Chan, and Z.Y. Liu, Phys. Rev. Lett. **80**, 956 (1998).
[32] R.W. Peng, M. Wang, A. Hu, S.S. Jiang, G.J. Jin, and D. Feng, Phys. Rev. B **57**, 1544 (1998).
[33] X.B. Yang, Y.Y. Liu, and X.J. Fu, Phys. Rev. B **59**, 4545 (1999).
[34] M.E. Zoorob, M.D.B. Charlton, G.J. Parker, J.J. Baumberg, M.C.

Netti, Nature (London) **404**, 740 (2000).
[35] D.H. Dunlap, H.L. Wu, and P.W. Philips, Phys. Rev. Lett. **65**, 88 (1990).
[36] H.L. Wu, W. Goff, and P. Phillips, Phys. Rev. B **45**, 1623 (1992).
[37] X.Q. Huang, Y. Wang, and C.D. Gong, J. Phys.: Condens. Matter **11**, 7645 (1999).
[38] X. Fu, Y. Liu, P. Zhou, and W. Sritrakool, Phys. Rev. B **55**, 2882 (1997).